Discrimination of Bird and Insect Radar Echoes in Clear-Air Using High-Resolution Radars

William J. Martin*

Center for Analysis and Prediction of Storms, University of Oklahoma, Norman, Oklahoma

Alan Shapiro

Center for Analysis and Prediction of Storms and School of Meteorology, University of Oklahoma, Norman, Oklahoma

Submitted to Journal of Atmospheric and Oceanic Technology

April, 2006

Revised August, 2006

Revised October, 2006

*Corresponding author address:

Dr. William Martin

Center for Analysis and Prediction of Storms

National Weather Center, Suite 2500

120 David L. Boren Blvd.

Norman, OK 73072

Phone: (405) 325-0402

E-mail: wjmartin@ou.edu

Abstract

The source of clear-air reflectivity from operational and research meteorological radars has been a subject of much debate and study over the entire history of radar meteorology. Recent studies have suggested that bird migrations routinely contaminate wind profiles obtained at night, while historical studies have suggested insects as the main source of such nocturnal clear-air echo. This study analyzes two cases of nocturnal clear-air return using data from operational WSR-88D radars and X- and W-band research radars. The research radars have sufficient resolution to resolve the echo as point targets in some cases. By examining the radar cross-section of the resolved point targets, and by determining the target density, it is found for both cases of nocturnal clear-air echo, that the targets are almost certainly insects. The analysis of the dependence of the echo strength on radar wavelength also supports this conclusion.

1. Introduction

Shortly after the invention of radar, radar echoes were received from optically clear air and scientists struggled to explain the source of these signals. Explanations for clear-air return have been controversial up until the present time. Excellent reviews of the early history of this problem are available from Battan (1973, Ch. 12) and Hardy and Gage (1990). Early explanations quickly focused on three potential sources for clear-air echoes: birds, insects, and refractive index gradients. Which of these three potential targets was the cause of clear-air echoes was debated. The controversy was thought to be settled for many cases by influential studies using the powerful Wallops Island radars which deduced that point targets were insects (and occasionally birds) while diffuse layer-echoes were caused by refractivity fluctuations (Hardy and Katz, 1969).

More recently, however, the possibility that migratory birds may be contaminating radar-derived wind profiles, especially at night, has become a concern. These concerns arose from experience with radar wind profilers (Wilczak et al. 1995; Jungbluth et al. 1995) from which large discrepancies between radar winds and winds obtained from balloon soundings were found. This discrepancy is largely confined to nocturnal clear-air. However, despite clear evidence that migratory birds can contaminate radar returns, it is not clear how widespread this contamination actually is. Indeed, there is ample evidence in the literature for both insects and birds being the dominant sources of clear-air echoes. Unfortunately, there is no simple, reliable method to discriminate bird from insect echoes. QC methods for radar winds may often flag radar data as contaminated by birds when the source of data is actually insects. For example, the research technique described by Zhang et al. (2005) for discriminating bird and insect targets from WSR-

88D data uses parameters derived from reflectivity and radial velocity patterns. For the data presented in Section 4, we have unequivocal evidence that the radar targets were almost entirely insects, but the QC criteria of Zhang et al. (2005) and Liu et al. (2005) would have flagged these data as bird-contaminated.

Ornithologists using radars typically assume their targets are birds, while entomologists typically assume they are insects. Because the target density for birds or insects needed to cause a strong radar echo is well below that which would be noticed visually, ground-truth is rarely available of the source of an echo. There may be times when presumed birds are actually insects and presumed insects are actually birds (see, for example, Larkin, 1991). For meteorologists, the discrimination of birds and insects matters because migratory birds are known to seriously bias wind measurements, while insects are believed to be less of a problem. It is only if the targets are moving by self-propulsion in a general direction that a bias would exist, and this is the case with bird migration. Alignment of migratory insects can also occur and is a potential problem, but would cause somewhat less bias due to the lower air speed of insects.

a. The diurnal cycle and general characteristics of clear-air echo

Clear-air return can occur as isolated targets or as layers or volumes filled with reflectivity. Isolated clear-air targets have been referred to as “ghosts”, “phantoms”, or, more commonly in papers from the 1930’s to 70’s, as “angels”. The term “angel” is used in the literature to refer to clear-air echoes in general, including volumetric, layer, and point echoes.

Clear-air reflectivity in the boundary layer has a pronounced daily cycle. Typically, it is weak during the day and confined below three kilometers. There is a strong dip in reflectivity and depth of echo at sunset, followed by a rapid increase in reflectivity and height of return after

sunset, beginning from the ground and moving upward. This rapid increase in clear-air return at sunset is often referred to as "radar bloom". Schaefer (1976) described radar bloom and interpreted it as being due to an impressive evening take-off of locusts and moths. The identical scenario was described by O'Bannon (1995), who believed it to be due to migrating birds taking off at sunset. Nocturnal return can reach 25 dBZ in exceptional cases, and is commonly 10 dBZ, comparable to the reflectivity of light rain. Nocturnal return typically decreases towards the end of the night followed by a rapid dip at sunrise, which is followed by a modest, but rapid increase to the daytime level.

Figure 1 shows a typical example of the daily cycle of clear-air reflectivity in the boundary layer as seen by a WSR-88D radar. This figure is a time-height cross-section obtained from KVNX (located in north-central Oklahoma) on one day in June, 2002. There was no precipitation within measurement range of the radar on this day. Volume scans were available every 10 minutes, and the time-height cross-section was calculated using the average reflectivity over the scan at each radial gate distance (and, therefore, height above the ground) from data with a 1.5° elevation angle. This angle was chosen as previous work (Martin and Shapiro 2005) found this elevation angle to suffer the least from ground-clutter contamination.

The local minima in reflectivity at sunrise and sunset are interesting features which are almost always seen when appreciable clear-air reflectivity is detected by WSR-88D radars. This phenomenon suggests a change in echo causing mechanism from day to night. Hardy and Glover (1966) suggested that this cycle could be due to insects of one species leaving the atmosphere at sunset while another enters it at night, though it could also conceivably be caused by different species of birds, or by a change in the refractivity structure of the boundary layer.

Sunrise and sunset are times of rapid changes in both bird and insect behavior and in the turbulent structure of the boundary layer.

There is a pronounced seasonal variation in clear-air return with return generally being stronger in the warm season. In the Great Plains, late spring seems to have the strongest clear-air return at night. Day-to-day values can fluctuate considerably, however, with reflectivity levels differing by 20 dBZ from one day to the next.

There are also strong day-to-day regional fluctuations. On one night, for example, the clear-air return might be strong over the Gulf Coast states and weak everywhere else in the United States, while on the next night, it might be strong over states in the upper Midwest and weak along the Gulf Coast. Clear-air return tends to be weak at locations west of the Rocky Mountains year round.

PPI scans of clear-air reflectivity sometimes show marked bilateral symmetry in which reflectivity is strongest in two directions 180˚ apart. This bilateral symmetry extends to polarization variables (Zrnić and Ryzhkov 1999; Land and Rutledge, 2004). This symmetry was noted by Shaefer (1976) and Riley (1975) who attributed it to insects aligned in the same direction. It was noted by Gauthreaux and Belser (1998) who attributed it to migrating birds being aligned.

Clear-air reflectivity displays from 88-D radars are often granular in presentation, implying fields of reflectivity consisting of a large number of discrete targets. The granularity is different between daytime and nighttime return (as seen in the VAD plots of Browning and Atlas 1966) with nighttime return having larger grains.

Clear-air reflectivity is usually very weak over large bodies of water. This effect is so marked that details of a coastline can often be discerned from the clear-air PPI display. For

example, it is common for the Melbourne, Florida WSR-88D to show 10 to 20 dBZ of reflectivity over land and no detectable reflectivity over adjacent coastal waters and Lake Okeechobee. Isolated spots of reflectivity over a body of water are sometimes seen over small islands. Sometimes, though, reflectivity is just as strong over water as over land.

Rings and lines of echo are also often seen. Thin lines on radar appear to be associated with a variety of wave phenomena and boundaries including fronts, drylines, gust fronts, and sea breeze fronts. The source of echo for such lines has been attributed to insects accumulating at meteorological boundaries (Geerts and Miao 2005a and 2005b; Russell and Wilson 1997, Wilson et al. 1994, Schaefer 1976). Thin lines of clear-air reflectivity are common in the Great Plains region. For reasons which have never been elucidated, these lines tend to be best defined (thinnest and sharpest) in the late afternoon. Nocturnal thin lines are most often seen associated with thunderstorm outflows. Daytime lines are more common than nocturnal lines, and are so numerous that it is not always clear what phenomenon they are related to. Expanding rings of clear-air return are seen at certain times of the year at sunset or sunrise. Elder (1957) first noticed these and suggested that they might be due to a shear-gravity wave. However, it is now recognized that these rings are almost certainly due to birds (at sunrise) or bats (at sunset) leaving roosting sites (Battan 1973, p. 258-9; Eastwood 1967, p. 165-181; Gauthreaux and Belser 1998).

Layers of clear-air return are also often seen, especially with long wavelength radars. These are often found to be co-located with inversions (Lane and Meadows 1963). Sometimes these layers are wrap-up into Kelvin-Helmholtz rolls. Reflectivity in these layers have often been attributed to insects by entomologists (Schaefer, 1976; Reynolds et al., 2005)

b. Birds

Ornithologists began studying birds with radar as early as 1945. Eastwood (1967), in a review of the early history of radar ornithology, accepts birds as the cause of most point-target angel echoes. Although ornithologists make some general statements about bird behavior, they also cite many exceptions. For example, Lowery and Newman (1966) reported a great variety of bird activity relative to fronts, prevailing winds, and daily behavior: birds sometimes fly with the wind, sometimes against the wind, and sometimes in opposite directions in nearby geographic regions.

Birds tend to be most active at sunrise and sunset. Migratory birds, which must move long distances, often travel at night, sometimes in flocks, but also individually or in small groups. The reasons birds behave as they do and how they navigate are topics of active research in the ornithological community. Birds should be detected by weather radars when present, though they may not fly at a high enough altitude and in large enough numbers to be a serious source of contamination. Most birds spend their lives less than 100 m above the Earth's surface. Shamoun-Baranes et al. (2006) by use of a tracking radar found that most birds flying during the day were below 200 m, with few as high as 1000 m.

NOAA's Environmental Technology Laboratory (ETL) considers migratory birds to be a significant problem and routinely flag as "bad" radar wind profiler data at night at low levels during certain months of the year when certain criteria are met (van de Kamp et al. 1997; Miller 1997; Wilczak et al. 1995). This is particularly unfortunate since wind profiler measurements of the low-level jet (LLJ) in the spring time are almost always so flagged. Similar quality-control schemes are in use for filtering WSR-88D winds by NCEP (Collins 2001).

The strongest evidence for the contamination of radar winds by the presence of migratory birds comes from balloon soundings simultaneous with radar-derived wind profiles which show radar-derived winds significantly different from those derived from balloons. These differences appear to occur only at night and during seasons when birds are expected to migrate. O'Bannon (1995) and Gauthreax et al. (1998) report on this discrepancy with WSR-88D VAD wind profiles and Wilczak et al. (1995) report on this problem with long wavelength wind profilers. These differences can be as much as 15 m s^{-1}, with the difference wind vector consistent in direction and amplitude with what would be expected if the radar was tracking migrating birds. Jain et al. (1993) examined this problem by comparing NSSL Cimarron radar VADs with CLASS soundings for a LLJ in May. They found radar winds stronger than the balloon sounding by about 4 m s^{-1} (as might be expected from contamination from large, aligned insects). They doubted birds could account for the discrepancy due to an unrealistically large number of birds needed to explain the presence of reflectivity throughout the depth and horizontal extent of the boundary layer. Instead, they blamed the discrepancy on the long sampling time and coarse vertical resolution of the CLASS system.

It is difficult to obtain observations of the numbers and altitudes of birds flying at night, and reports of the actual presence of birds during times when radar winds are in error have rarely been reported. A standard method of counting birds at night is to observe moon crossings of birds through a telescope, from which traffic rates can be deduced. Gauthreaux and Belser (1998) have correlated such bird counts with WSR-88D reflectivity levels. There is, however, a great deal of scatter in this correlation, and moon crossings do not give any information on the altitude of the birds.

c. Insects

Similar to radar ornithology, the field of radar entomology developed practically from the beginning of radar. As early as 1949, Crawford (1949) identified insects as the cause of most, if not nearly all, angel echoes. Schaefer (1976) and Riley (1989) provide reviews of radar entomology. Most insects stay close to the Earth's surface when under self-directed flight. Insects which fly at high altitudes primarily migrate with the ambient wind, which is typically much faster than insect air speeds. As long as insects are not aligned, they pose little threat to radar wind measurement accuracy. However, insect alignment can add as much as 5 m s^{-1} to radar winds. Alignment of insects was surmised by Riley (1975) from the presence of a bilaterally symmetric PPI echo pattern. Comparison of a pilot balloon with radar tracks indicated that the targets were moving against the wind with an air speed of about 5 m s^{-1}. Large insects such as grasshoppers and moths are more likely to fly at night at altitude and are more likely to be aligned in flight than are smaller insects (or "aerial plankton") which often populate the boundary layer during the day.

Drake (1984, 1985) studied the presence of insects in a LLJ in Australia. He observed bilaterally symmetric PPI patterns and also noted the rapid increase of reflectivity at dusk, which he attributed to a mass take-off of large insects (moths). The large number of echoes and the calculated radar cross-section of 1 cm^2, plus the trapping of some insects at altitude, convinced Drake that most of his echoes were insects. By using airborne traps, Berry and Taylor (1968) confirmed the presence of aphids to an altitude of 610 m at night in Kansas, also in a LLJ.

Sometimes strong clear-air reflectivity events are noticed at the same time as the appearance of unusual numbers of air-borne insects. For example, Hardy and Katz (1969) report

on Benard-like cells seen in clear-air during the daytime with unusually high reflectivity at the same time as an abnormal number of airborne ants were observed.

Influential studies conducted at Wallops Island in the mid 1960's compared the clear-air reflectivity patterns obtained simultaneously with radars of different wavelengths (3 cm, 11 cm, and 71 cm; Hardy and Katz 1969). These experiments showed a wavelength dependence of the strength of echo for different kinds of clear-air return. Reflectivity associated with dot echoes in the lower troposphere was found to decrease at longer radar wavelengths. This is what is expected for scattering from objects smaller than the wavelength of the radar. Such Rayleigh scattering has an inverse dependence on the fourth power of wavelength. This supported the view that the scatters were small objects, probably insects. Thin reflectivity layer echoes, on the other hand, were observed to be stronger at the longer wavelengths. This dependence was shown to be quantitatively consistent with scattering from index of refraction gradients modified by turbulence (Bragg scatter), which has an inverse dependence on the 1/3 power of wavelength. As a result of these experiments, dot echoes were firmly believed to be due to insects or birds. More recent work by Wilson et al. (1994) came to the same conclusion that most daytime clear-air return is due to insects. Gossard (1990) using high-resolution radar images, attributed dot echoes throughout the boundary layer to insects.

d. Refractive Index Gradients

Friend (1939), using a vertically pointing radar with an A-scan display found strong reflectivity layers in the lower troposphere co-located with temperature inversions. He attributed the echoes to reflections of radar energy from gradients in the dielectric constant of the propagating medium (or, equivalently, gradients in the index of refraction). However, later

calculations of what gradients were required to account for the observed reflectivity indicated that the necessary gradients were on the order of 20 N-units per centimeter (Battan 1973, p. 255). Doubts about whether such large gradients could actually exist led to the acceptance of the theory of turbulent Bragg scatter (sometimes also referred to as "Refractive Index Turbulence (RIT)" or turbulence scatter). Bragg scatter theory makes numerous assumptions and approximations (Tatarski, 1961); nevertheless, good agreement was obtained by several researchers between predicted reflectivity and that observed with radars of various wavelengths (Kropfli et al. 1968).

In Bragg scatter theory, interference of the radar energy scattered from a random turbulent refractivity field, leads to only reflections from turbulent eddies about the size of half the radar wavelength ultimately contributing to the received signal. The Bragg scatter theory results in an expression for the backscatter energy from turbulent eddies as a function of the amount of turbulence, the mean refractive index gradient, and the radar wavelength. Bragg scatter is theoretically much stronger than reflections from refractive index discontinuities, and can account for echo which fills a volume of space.

e. This study

This study looks at two cases of clear air return in the lowest several kilometers of the atmosphere using radars of sufficient resolution to separate bird or insect echoes as point targets. The cases are of strong clear-air return in the entire volume of the boundary layer at night. WSR-88D data were available for comparison. The value of the high resolution radars is that they can determine the radar cross-section of individual targets, as well as allow the targets to be

counted. The measured radar cross-sections and target densities can then be compared with what would be expected from birds and insects so that these targets can be discriminated.

2. Radar equations

What is commonly referred to as the "weather radar equation" takes various forms, but generally relates the received power at the antenna to radar and target parameters. What is commonly recorded in radar data is the radar reflectivity factor, Z, in units of $mm^6\ m^{-3}$; usually recorded as decibels, dBZ = 10 log Z. The definition of Z arises from the Rayleigh scattering approximation. For Rayleigh scattering, the radar targets are small relative to the radar wavelength, and the radar backscatter cross-section for a single water sphere is:

$$\sigma_{Ray} = \frac{\pi^5}{\lambda^4}\left|K\right|^2 D^6, \qquad (1)$$

where σ_{ray} is the backscatter cross-section (σ) for Rayleigh scatter, λ is the radar wavelength, K is the complex index of refraction of water ($\left|K\right|^2 \approx .93$), and D is the drop diameter. Z is then defined as a sum over all the radar targets in the radar probe volume as:

$$Z = \frac{\sum_i D_i^6}{Vol.} = \frac{\lambda^4}{\pi^5\left|K\right|^2}\frac{\sum_i \sigma_{Ray_i}}{Vol.}. \qquad (2)$$

The radar equation then takes the form (Probert-Jones, 1962):

$$P_r = \frac{P_t G^2 \lambda^2 \theta^2 hL}{1024(\ln 2)\pi^2 r^2}\frac{\sum_i \sigma_i}{Vol.} = \frac{P_t G^2 \theta^2 Lh\pi^3\left|K\right|^2}{1024(\ln 2) r^2 \lambda^2} Z, \qquad (3)$$

where P_r is the received power, P_t is the transmitted power, G is the antenna gain, θ is the beam width, h is the pulse length, L is a loss factor, r is the range to the center of the probe volume, and σ_i is the backscatter cross-section of the i^{th} target. This equation is converted to decibels and

solved for reflectivity in dBZ. For cases where the scattering targets are not Rayleigh scatterers (or water spheres), reported Z values are effective reflectivity factor values, Z_e.

If the radar target is, in fact, a single scatterer (located near the beam center), then the received power is (Probert-Jones 1962):

$$P_r = \frac{P_t G^2 \lambda^2 L}{(4\pi)^3 r^4} \sigma . \qquad (4)$$

For the case where there is a single point target in the radar beam, the radar backscatter cross-section can be deduced from reported Z values by equating (3) with (4), yielding:

$$\sigma = 80.6 \frac{r^2 \theta^2 h}{\lambda^4} Z_e . \qquad (5)$$

The equation for effective reflectivity due to Bragg scatter was derived by Silverman (1956) and Tatarski (1961):

$$Z_e = .0013 C_n^2 \lambda^{\frac{11}{3}} , \qquad (6)$$

where C_n^2 is the refractivity structure parameter.

3. Characteristics of WSR-88D, DOW3, and UMASS radars

a. Radars

This study uses data from 3 WSR-88D radars of the NEXRAD program (Klazura and Imy 1993; namely KVNX (for Fig. 1), and KGLD and KTLX), as well as data from the Doppler on Wheels (DOW3) radar (Wurman et al. 1997; Wurman 2001) and the University of Massachusetts' (UMASS) 3 mm mobile radar (Bluestein and Pazmany 2000). Selected characteristics of these radars are given in Table 1. As this study wishes to determine radar

cross-sections of targets (potentially insects or birds), knowledge of the accuracy of the calibration is necessary, as well as some consideration of the relevant scattering regime for targets of varying size.

b. Calibration of WSR-88D, DOW3, and UMASS radars

WSR-88D radars record data in level II format (Crum et al. 1993), the rawest format routinely archived, to a discretization of 0.5 dBZ. These radars are calibrated to within 1 dBZ by using internal reference signals. This is done by using a radio-frequency pulse that is injected into the receiver every volume scan. Since such calibration checks do not account for antenna gain or loss over time, it is possible that some WSR-88D radars may not be in accurate calibration. It is not normally possible to know the magnitude of such system losses. Absent knowledge of equipment problems, WSR-88D data will be assumed here to be accurate to ± 1 dBZ.

DOW3 has not been calibrated by reference signals or by reference targets. It is possible to calculate what the calibration should be theoretically based on known radar characteristics by using the radar equation. In logarithmic form, the radar equation (3), after assuming $G = \frac{\pi^2}{\theta^2}$ (approximate for a circular paraboloid antenna), and converting to convenient units is:

$$P_r = -128.9 + 10\log\frac{P_t h}{\theta^2 \lambda^2} + dBZ - 20\log r - system\ losses\,, \qquad (7)$$

where P_r is in dBm, P_t is in watts, θ is in degrees, λ is in cm, h is in meters, r is in km, and Z is in $mm^6\ m^{-1}$. Calibration determines the system losses so that the target reflectivity can be found from (7). Wurman (personal communication) has suggested using a pessimistic 5 dB for system losses for DOW3. A guess for system losses could miss some equipment problems. For

example, bad wave-guide connections or a malfunctioning transmitter could lead to a grossly erroneous calibration. Nonetheless, consistency of radar operation during the season the data considered here were collected (e.g., that radar echoes of certain phenomena are similar to those expected by the radar operator) leads to some confidence that this theoretical calibration is reasonable; accordingly, we will use a precision of ±3 dB for DOW3 (or a factor of two for power levels in watts) and 5 dB for system losses.

The UMASS radar was calibrated using a reference target (a corner reflector) after the completion of the 2001 data collection season (Pazmany, personal communication). The calibration was found to be accurate to within 1 dB and stable at that time.

c. Mie scattering

For insect and bird targets, the Rayleigh scatter approximation is inaccurate for the radars considered here. Consequently, Mie scattering calculations are necessary. Mie scattering calculations can give the correct radar cross section for any object at any radar wavelength. The equations for scattering from spherical objects were derived first by Mie in 1908 and have been studied in great detail by others since. Computer codes for the lengthy and tedious Mie scatter calculations are widely available. This work uses a code obtained from NASA/Goddard and described in Wiscombe (1979, 1980). The input to the Mie scattering algorithm includes the complex index of refraction of the scatterer (assumed to be water spheres), which depends on the radar wavelength and water temperature. Values for this study were taken from Gunn and East (1954) for 10 cm and 3.21 cm wavelengths, assuming an air temperature of 20˚C, and from Lhermitte (1990) for a 3.2 mm wavelength. These wavelengths are very close to those of the

radars used for this study, and may be used for this study because the index of refraction is not a strong function of wavelength at microwave frequencies.

Radar cross-sections from Mie scatter calculations for a range of drop size and for the three radars are shown in Fig. 2. On this figure are plotted for reference the letters 'R', 'I', and 'B' at locations corresponding to the approximate equivalent water sphere sizes for rain drops, insects, and birds (Vaughn 1985). Also plotted in Fig. 2 are three parallel solid lines which are the Rayleigh scattering values from (1), and another solid line crossing the parallel lines which is the so-called "optical limit" line. This is the line for which the radar cross section equals the drop cross-section. For large drop radii, the radar cross-section from Mie calculations is a little below the optical limit due to absorption of energy.

4. Analysis of the clear-air echo under nocturnal conditions

a. Goodland, KS: WSR-88D and DOW3

On 30 May 2000, DOW3 was co-located with the KGLD WSR-88D at the Goodland, Kansas Weather Service Office from 0500-0700 UTC (around midnight); DOW3 being parked within 100 m to the south of KGLD. Moderately strong clear-air return was seen by KGLD and DOW3 in the lowest 2 km of the atmosphere. At this time, a squall line had passed off to the north and was far enough away that KGLD was put into clear-air mode at about 0530 UTC. A strong low-level jet had developed with winds to 32 m s^{-1} (according to KGLD) with strong clear-air reflectivity to 10 dBZ (also according to KGLD). Data were collected for analysis in an attempt to discern the source of echo. Analysis of the wind profile obtained from this data set and ground clutter contamination problems are discussed in Martin and Shapiro (2005).

Figure 3 (left) is the PPI scan of reflectivity from KGLD for a tilt of 2.5° at about 0556 UTC and Fig. 3 (right) is the corresponding PPI from DOW3 obtained within one minute of Fig. 3 (left). These figures are plotted with height range rings drawn every 200 meters above the surface. The usage of a height range scale is different from conventional displays in which the rings are usually the horizontal or slant range from the radar. This is done to facilitate analysis of the vertical profile of reflectivity; it is more useful to know how far above the ground the echo is than how far away it is in range. Both panels of Fig. 3 depict the same tilt for both radars, at the same time, and are plotted on the same scale. The polarization of both radars is also the same (horizontal). The only difference is the gray scale. Because DOW3 had a reflectivity about 15 dBZ lower than KGLD, it was necessary to plot on a gray scale 15 dBZ below that of KGLD. Other differences are due to the peculiarities of the radars. DOW3 shows some beam blockage to the north (top of figure) from the NWS office and KGLD tower. The radial resolution of DOW3 was also superior, with a 137 m gate spacing, versus 1000 m for KGLD. Also, while the angular beam size is the same for both radars at 0.95°, DOW3 was over-sampling, obtaining a radial of data every 0.2°, versus every degree for KGLD.

That DOW3 reported reflectivity significantly weaker than that of KGLD is an important clue to the nature of the echo. This rules-out Rayleigh scatterers as the source of echo, as these would not show any dependence on wavelength. The difference in dBZ_e that two wavelength radars would be expected to have if Bragg scatter was the cause of echo from (6) is:

$$\Delta dBZ_e = \frac{110}{3} \log \frac{\lambda_1}{\lambda_2}. \qquad (8)$$

For insect and bird targets, this difference can vary from none for small insects in Rayleigh scatter to a value approximated by the optical limit in which σ is approximately the actual cross section of the target. Equation (5) then implies a maximum difference of:

$$\Delta dBZ_e = 40\log\frac{\lambda_1}{\lambda_2} - 20\log\frac{\theta_1}{\theta_2} - 10\log\frac{h_1}{h_2}, \qquad (9)$$

for Mie scatters, with Fig. 2 potentially being used to find the actual difference if the size of the scatterers was known. Given the 10.0 cm wavelength for KGLD and the 3.20 cm wavelength of DOW3, plus the beam widths of about 0.95˚ for both radars and the pulse length of 471 m for KGLD (VCP 32) and 274 m for DOW3, these equations imply that, for Bragg scatter, we would expect ΔdBZ_e=18 dB; and for birds and insects, we would expect ΔdBZ_e = 0 to 17 dB.

To analyze the difference in this case, the reflectivity is averaged over the box drawn to the southwest of the radars in Fig. 3. This location is about 1.1 km above the surface (a range of 25 km), and both radars are sampling approximately the same air at the same time. For DOW3, the signal is not continuous and the average is taken only counting those data above the noise level. It is found that DOW3 had an average reflectivity factor within the box of -14 dBZ, while KGLD had -3 dBZ. Given the 1 and 3 dB calibration uncertainties for KGLD and DOW3 respectively, this gives:

$$\Delta dBZ_e\ (observed) = 11 \pm 4\, dB$$

This value is not consistent with a Bragg scatter or large bird explanation, unless other errors can account for another 3 dB of error. It is consistent with insects of large enough size, or possibly small birds, and is similar to the 7 dB difference between X- and S-band radars found by Wilson et al. (1994) for similar echo.

Figure. 4 is a reflectivity PPI scan of higher resolution DOW3 data acquired at a 10° tilt about 10 minutes after Fig. 3. These data are of the highest possible resolution attainable by DOW3, with a gate spacing of 12 m. Figure 4 shows the lowest 500 m of air to a range of 3 km. The numerous point targets evident in this figure imply either an insect or bird explanation. Data from numerous studies on the radar cross-section of birds and insects (Vaughn 1985; Riley 1985;

Eastwood 1967), combined with (5) imply that at a range of 2 km, and with a 12 m gate spacing, DOW3 would indicate the effective dBZ levels and radar cross-sections listed in Table 2 for a single bird or insect in the probe volume. The reflectivity factor of the point targets in Fig. 4 is about 5 to 12 dBZ at a range of 2 km. This corresponds to a radar cross section (from (5)) of from 0.06 to 0.32 cm^2, which corresponds to values typical of insects, but is low for birds.

That the source of echo was a distribution of point targets might also have been deduced from the lower resolution data of Fig. 3 (right). This figure has a granularity to it, implying that the target density is insufficient to fill every resolution volume with at least one target. Since Bragg scatter is expected to be volume filling, it should give a spatially continuous signal. Granularity is an excellent indication of point targets such as birds or insects. However, a spatially continuous echo does not rule out bird or insect scatterers, as the density of such targets can be quite high. If birds were present, they must have been few in number since none of the point targets of Fig. 4 have a radar cross-section much greater than 2 cm^2.

An RHI scan at the same location as Fig. 4 at the same 12 m gate spacing at a time about 20 minutes earlier is shown in Fig. 5. Here it is seen that the point targets extend up to 2 km in elevation, though they are most numerous below 1 km. Fig. 5 also indicates a nearly continuous signal in the shallow layer 200 m above the surface. Point targets are still obvious in this layer, but they are surrounded by much weaker echoes. The reflectivity at a range of 2.5 km of the weak echo in this shallow layer is about -12 dBZ. This corresponds to a radar cross-section of 2×10^{-3} cm^2, consistent with very small insects. Possibly this layer of air has a very high population of very small insects. Alternatively, this weak reflectivity could be due to Bragg scatter, since a layer of air near the ground at night might have a strong mean vertical refractivity gradient caused by radiational cooling.

The number density of point targets in Fig. 4 can be estimated and it is instructive to compare this estimate with ornithological bird migration censuses. To estimate the number density, we count the number of targets over a large sector of Fig. 4 and divide by the volume of the sector:

$$Vol. = \int_{\phi-\Delta\phi/2}^{\phi+\Delta\phi/2} \int_{0}^{\Delta\theta} \int_{r}^{r+\Delta r} r^2 \cos\phi \, dr d\theta d\phi , \qquad (10)$$

where r is the radial distance, θ is the azimuthal direction, ϕ is the elevation angle, and $\Delta\phi$ is the beam width. This integration yields the formula:

$$Vol. = \frac{4}{3}\pi^2 \cos\phi [(r+\Delta r)^3 - r^3] \frac{\Delta\theta\Delta\phi}{360^2} , \qquad (11)$$

which assumes $\sin(\Delta\phi) \approx \Delta\phi$ and that the angles are measured in degrees. This leads to an estimate of 5.0 X 10^{-6} targets per cubic meter, or an average of one target per 60 meter cube. To put this in perspective, if this concentration was the case for all the air below 1 km for the entire state of Kansas, it would imply almost 1 billion birds flying overhead at that time in Kansas, if the targets were birds.

Bird density during migration is measured in terms of the number of bird crossings per mile (1610 m) of front per hour, and is referred in the ornithological literature as "migration traffic rate" (MTR) or "flight density" (Lowery and Newman 1966). Given the 5.0 X 10^{-6} targets per m^3 seen in these data, and the average 25 m s^{-1} ground speed of the wind profile below 1 km for this case (Martin and Shapiro 2005), the calculated MTR is 7.3 X 10^5 birds per 1610 m per hour. In a study utilizing 265 observing stations across the country, Lowery and Newman (1966) measured MTR throughout the country (with the help of 1391 observers) on 4 nights in October of 1952. Bird counts were accomplished by watching birds cross the visible moon through a telescope and applying complex formulas to arrive at MTR values. Lowery and Newman (1966)

note various problems with this technique. Their data reduction task was so complex, it took over a decade to accomplish. They found typical migration rates of about 3700, with 4500 being "heavy". This is a factor of 160 less than the traffic rate seen here. Gauthreaux et al. (1998) reports MTR values obtained by moon-watching along the U.S. Gulf Coast, an area which can have particularly intense migratory traffic. The maximum MTR value they reported was about 200 000 (with more typical values of 20 000), still 1/3 that observed with these data. MTR values as high as those implied by a bird explanation for the echo analyzed here would not be expected to exist over a very wide area.

The combination of radar cross-sections consistent with insects, and the number density of scatterers vastly exceeding what would be expected from migratory birds, strongly argues against birds being a significant source of radar echo in this case.

b. Norman, OK: WSR-88D and UMASS

To further study the source of clear-air echoes, radar data were acquired on the night of 19 May 2001 at about 0400 UTC at the Max Westheimer Airport in Norman, Oklahoma under clear-air nocturnal conditions. The UMASS W-band radar was used. This radar has exceptional spatial resolution with a beam width of 0.18° and a pulse length of 60 m. Over-sampling in the radial direction is accomplished with a gate spacing of 15 m. Three millimeters is an unusual wavelength for meteorological applications, and use of this radar presented some special problems. One difficulty is that the near-field of the radar extends out to 900 m. As the radar is designed with an intended range of less than 10 km, many of the radar targets will be in the near field. This problem is dealt with by replacing r for short ranges in the standard radar equations with D/θ, with θ the beam width and D the antenna diameter. Another problem is attenuation.

W-band radars suffer significant atmospheric attenuation due to absorption by oxygen. At the 3 mm wavelength, two-way attenuation near the earth's surface is about 0.7 dB per km (Fig. 42 of Blake 1970). This amount is added to the observed reflectivity values to correct for attenuation.

There was no nearby precipitation on this night or on the previous day. Figure 6 shows a PPI display of reflectivity at a tilt of 1.5° obtained from the KTLX WSR-88D radar. The KTLX radar was the closest WSR-88D radar to the UMASS radar, about 25 km away. Figure 6 indicates a very high reflectivity for clear-air, up to 25 dBZ in many areas, and at least 5 dBZ at all elevations below about 2.2 km. This is much stronger than the echo seen in Goodland, Kansas, discussed in the previous section. A wind profile derived by VAD analysis of the radial velocity data is present in Fig. 7. The velocities are fairly weak, about 6 m s^{-1} below 1 km, reaching 12 m s^{-1} at 3 km above the ground.

Figure 8 is a time-height display of reflectivity obtained by UMASS within 5 minutes of the data of Fig. 6. The UMASS radar antenna was pointed vertically and obtained 2414 radials of data over 195 seconds. Figure 8 shows a total depth of 3 km and many targets passing through the beam. Targets are seen below about 2.6 km, in good agreement with the depth of echo seen by KTLX. It should be noted that the radar beam is much wider at the upper levels, so that, if the time-height display shows about the same target density at all levels below 2.2 km, this implies a lower density of targets aloft. It is also instructive to note that fewer targets are seen in the layer near 1 km altitude than at other levels. This is most likely due to the weaker winds at this level causing individual insects to spend more time in the radar beam as they drift by, and agrees well with the weak winds in the wind profile at this level seen in Fig. 7. Radar cross sections for the strongest echoes around l km elevation (-16 dBZe) are about 0.2 cm^2, calculated from (5). The strongest targets near 2 km vertical range appear to be larger, with a

cross-section of 0.5 cm^2. There are no echoes at any level indicating a cross-section larger than 1 cm^2. This small cross-section is consistent with the presence of insects. Estimating the target density is straightforward. The number of targets in the radar beam below 2.2 km is counted by computer for each radial, and this number is divided by the beam volume through a depth of 2.2 km. This count gives an average of 2.7 targets in the beam at any given time, implying a target density of 1.0 X 10^{-4} per m^3. This is 20 times that seen at Goodland. Figure 2 implies that radar cross-section values above about 0.1 cm^{-2} are broadly similar at 3 mm and 10 cm. So using the UMASS number density times a representative radar cross section of 0.1 cm^2 implies by (2) a KTLX reflectivity of about 25 dBZ_e, in reasonable agreement with that observed.

Near 2 km in elevation, UMASS recorded reflectivity of about -15 dBZ, while KTLX values averaged about 10 dBZ. This is a difference of 25 dB. The expected difference from Bragg scatter or from very large birds would be by (8) and (9) about 61 dB. This further argues against a Bragg scatter or bird explanation. The very high target density and radar cross section typical of insects, again argues strongly that the targets are mostly, if not entirely, insects.

5. Summary and discussion

a. Findings from high-resolution radar studies

A combination of low radar cross-section and large number density of targets lead to the conclusion that the targets in both cases were almost certainly insects, with not a single bird being clearly identified. The difference in reflectivity between the two different radar wavelengths for each study was much smaller than that expected for birds, which further supports this conclusion. This is in agreement with the results of Wilson et al. (1994) and previous conclusions from entomologists and radar meteorologists that insects are the most

common cause of clear-air echoes. While there are undeniably times when significant bird-contamination of WSR-88D winds occurs in the Great Plains and elsewhere, the extent of the problem is unclear, as both cases looked at in detail in this study found only insects. It is possible that some geographic locations, such as the U. S. Gulf Coast, could have a larger problem with bird contamination than others due to a higher rate of bird migration.

The measurements also lead to the conclusion that Bragg scatter was not the cause of nocturnal return, as Bragg scatter would be expected to be spatially continuous, whereas what was found were point targets. However, some continuous weak reflectivity echo was seen below 200 m at Goodland which could conceivably have been due to Bragg scatter.

b. Discussion on the discrimination of bird and insect radar echo

Discriminating between birds and insects as the dominant cause of clear-air return is a critical and unresolved issue. Migrating birds on some occasions have been shown to almost certainly significantly bias radar wind estimates, while insects have not been shown to cause such serious bias. This is because of the significantly higher air speed of birds relative to insects. Aligned birds generate wind errors typically of 10 to 15 m/s. Aligned large insects might generate a bias as high as 6 m/s, and might be a problem in some cases, though this has never been confirmed. Effects from small insects are probably negligible. Knowledge of bird behavior is of limited help in this discrimination. While there are well-established patterns of bird behavior, there are numerous exceptions as well.

One tool for discrimination is the radar cross-section of birds and insects. Birds can be ruled out in some cases simply if the reflectivity is too low. A reflectivity threshold can be based on a minimum expected radar cross-section for birds. Vaughn (1985) combines studies of birds

and insects using radars with wavelengths from 0.86 to 75 cm and finds a range of cross-section from 0.1 to 1000 cm^2 for birds. However, most birds are between 1 and 100 cm^2, and from Eastwood (1967), passerine birds (the most common nocturnal migrants) have cross-sections of 10 to 30 cm^2. It might, therefore, be reasonable to use 10 cm^2 as a bird threshold. Insects, as shown here, can be found in high enough concentrations to explain high reflectivity levels, so, while low reflectivity can rule-out birds, high reflectivity does not rule out insects.

A spatially granular reflectivity or velocity pattern in a PPI display implies a density of targets below the density of resolution volumes. In such cases, it would be expected that each resolution volume would have few targets present at one time. In this case, high reflectivities would confirm the presence of birds. This technique can be used to confirm the presence of birds in Fig. 1 of Gauthreaux and Belser (1998). It might also be possible to exclude birds on the grounds that the number density needed to cause a spatially continuous reflectivity signal is excessive. Zhang et al. (2005) use granularity as one criterion to identify the presence of birds in WSR-88D data, though granular signals can be caused by insects.

One possibility for discrimination is to use the symmetry of the PPI echo pattern. The radar cross-section of a bird is 15 dB weaker when scanned head or tail on, than when it is scanned broadside. When aligned migratory birds are present, the radar should indicate much lower reflectivity when scanning in the direction of alignment. This would give a bilaterally symmetric PPI pattern as has sometimes (though not often) been reported (for example, Fig. 2a of Gauthreaux and Belser, 1998, and Lang et al., 2004). This phenomenon is also true for insects (Vaughn 1985); however, insect alignment in flight may show some differences in this effect. In any case a lack of aligned targets implies a lack of wind bias.

Another possible way to distinguish between bird and insect radar echoes is to use polarization information as explored by Zrnić and Ryzhkov (1998), Mueller (1983), and Zhang et al. (2005). Zrnić and Ryzhkov found what they believe to be a characteristic signature of differential reflectivity, Z_{DR}, and differential phase which is markedly different for birds and insects. Their technique is a potentially valuable tool for confirming the presence of birds, especially, as they state, since the polarization parameters do not depend on target concentration. However, they only analyzed one case of presumed birds and one of presumed insects. Also, Zrnić and Ryzhkov found Z_{DR} to be higher for presumed insects than for presumed birds, while Mueller (1983) found the opposite for the two cases he analyzed. As there are many species of insects with a wide range of length to width ratios, it may not be possible to distinguish birds and insects in all cases using polarimetric measures.

Bachmann and Zrnić (2005) have shown the ability to separate the velocity measurements from birds and insects using the Doppler spectra. This method is applicable only when both insects and birds are present in sufficient numbers to give separate peaks in the velocity spectra. If only one peak in the velocity spectrum is discernible, then it is not knowable from the spectra alone if the scattering targets are birds or insects. However, this method might be effective for longer wavelength wind profilers which are sensitive to Bragg scatter (Pekour and Coulter 1999) as an accurate air signal will be present from which a second spectral peak due to migrating birds could be discerned.

If a radar can be operated in tracking mode, then the wing beats of the target can be discerned. As wing beat patterns of birds and insects differ, this can be used for the discrimination of birds and insects (Larkin, 1991). Another method might be to consider temperature as insects will rarely be found airborne at temperatures below 5˚C.

Acknowledgements

The authors gratefully acknowledge the assistance of Josh Wurman for access to the DOW3 radar, and Andy Pazmany for access to the UMASS radar. This work benefited from discussions with Dick Doviak, Dusan Zrnić, and Doug Lilly. Also, Jeanette Bider and Gary Schnell provided valuable discussions and information on the habits of birds.

This research was supported by the Coastal Meteorological Research Program (CMRP) under Grant N00014-96-1-1112 from the United States Department of Defense (Navy), by the Center for the Analysis and Prediction of Storms (CAPS) under grant ATM91-20009 from the National Science Foundation, by the NSF IHOP program under NSF grant ATM01-29892, and by the University of Oklahoma. This research was also supported in part by the Engineering Research Centers Program of the National Science Foundation under NSF Award Number 0313747. Any opinions, findings, conclusions or recommendations expressed in this study are those of the authors and do not necessarily reflect those of the National Science Foundation.

References

Bachmann, S. and D. Zrnić, 2005: Spectral polarimetry for identifying and separating mixed biological scatters. *32nd Conference on Radar Meteorology*, Albuquerque, NM, Amer. Meteor. Soc.

Battan, L. J., 1973: *Radar Observations of the Atmosphere.* University of Chicago Press, 324 pp.

Berry, R. E. and L. R. Taylor, 1968: High altitude migration of aphids in maritime and continental climates. *J. Animal Ecol.*, **37**, 713-722.

Blake, L. V., 1970: Prediction of radar range. *Radar Handbook,* M. I. Skolnik, Ed. McGraw Hill Book Company, 2.1-2.73.

Bluestein, H. B. and A. L. Pazmany, 2000: Observations of tornadoes and other convective phenomena with a mobile, 3-mm wavelength Doppler radar: the spring 1999 field experiment. *Bull. Amer. Meteor. Soc.,* **81**, 2939-2951.

Browning, K. A. and D. Atlas, 1966: Velocity characteristics of some clear-air dot angels. *J. Atmos. Sci.*, **23**, 592-604.

Collins, W. G., 2001: The quality control of velocity azimuth (VAD) winds at the National Centers for Environmental Prediction. Preprints, *11th Symposium on Meteorological Observations and Instrumentation*, Albuquerque, NM, Amer. Meteor. Soc.

Crawford, A. B., 1949: Radar reflections in the lower atmosphere. *Proceedings of the I.R.E.*, **37**, 404-405.

Crum, T. D., R. L. Alberty, and D. W. Burgess, 1993: Recording, archiving, and using WSR-88D data. *Bull. Amer. Meteor. Soc.*, **74**, 645-653.

Drake, V. A., 1983: Collective orientation by nocturnally migrating Australian plague locusts, *chortoicetes terminifera* (Walker) (orthoptera: acrididae): a radar study. *Bull. Ent. Res.*,

73, 679-92.

Drake, V. A., 1984: The vertical distribution of macro-insects migrating in the nocturnal boundary layer: a radar study. *Bound. Lay. Meteor.,* **28**, 353-374.

Drake, V. A., 1985: Radar observations of moths migrating in a nocturnal low-level jet. *Ecol. Entomol.*, **10**, 259-265.

Drake, V. A. and R. A. Farrow, 1988: The influence of atmospheric structure and motions on insect migration. *Ann. Rev. Entomol.,* **33**, 183-210.

Eastwood, E., 1967: *Radar Ornithology.* Methuen & Co., Ltd. 278 pp.

Elder, F. C., 1957: Some persistent "ring" angels on high-powered radar. Proceedings*, Sixth Weather Radar Conference*. Cambridge, MA, Amer. Meteor. Soc.

Friend, A. W., 1939: Continuous determination of air-mass boundaries by radio. *Bull. Amer. Met. Soc.*, **20**, 202-205.

Gauthreaux, S. A. and C. G. Belser, 1998: Displays of bird movements on the WSR-88D: patterns and quantification. *Wea. And Fore.,* **13**,453-464.

Gauthreaux, S. A., D. S. Mizrahi, and C. G. Belser, 1998: Bird migration and bias of WSR-88D wind estimates. *Wea. And Fore.,* **13**,465-481.

Geerts, B. and Q. Miao, 2005a: The use of millimeter Doppler radar echoes to estimate vertical air velocities in the fair-weather convective boundary layer. *J. Atmo. Oceanic. Technol.*, **22**, 225-46.

Geerts, B. and Q. Miao 2005b: A simple numerical model of the flight behavior of small insects in the atmospheric convective boundary layer. *Environ. Entomol.*, **34**, 251-72.

Gossard, E. E., 1990: Radar research on the atmospheric boundary layer. *Radar in Meteorology,* David Atlas Ed., Amer. Meteor. Soc., 477-527.

Gunn, K. L. S. and T. W. R. East, 1954: The microwave properties of precipitation particles. *Quart. J. Roy. Meteor. Soc.*, **80**, 522-545.

Hardy, K. R., and K. M. Glover, 1966: 24 hour history of radar angel activity at three wavelengths. Proceedings, *Twelfth Conference on Radar Meteorology*, Norman, OK, Amer. Meteor. Soc.

Hardy, K. R. and K. S. Gage, 1990: The history of radar studies of the clear atmosphere. *Radar in Meteorology,* David Atlas, Ed., Amer. Meteor. Soc., 130-142.

Hardy, K. R. and I. Katz, 1969: Probing the atmosphere with high power, high resolution radars. *Proceedings of the IEEE*, **57**, 468-480.

Jain, M., M. Eilts, K. Hondl, 1993: Observed differences of the horizontal wind derived from Doppler radar and a balloon-borne atmospheric sounding system. Preprints, *8th Symposium on Meteorological Observations and Instrumentation*, Anaheim, CA, 189-194.

Jungbluth, K., J. Belles and M. Schumacher, 1995: Velocity contamination of WSR-88D and wind profiling data due to migrating birds. Preprints, *27th Conference on Radar Meteorology*, Vail, CO, Amer. Meteor. Soc.

Klazura, G. E. and D. A. Imy, 1993: A description of the initial set of analysis products available from the NEXRAD WSR-88D system. *Bull. Amer. Meteor. Soc.,* **74**, 1293-1311.

Kropfli, R. A., I. Katz, T. G. Konrad, and E. B. Dobson, 1968: Simultaneous radar reflectivity measurements and refractive index spectra in the clear atmosphere. *Radio Sci.*, **3**, 991-994.

Lane, J. A. and R. W. Meadows, 1963: Simultaneous radar and refractometer soundings of the troposphere. *Nature*, **197**, 35-36.

Lang, T. J., S. A. Rutledge, and J. L. Stith, 2004: Observations of quasi-symmetric echo patterns in clear air with the CSU-CHILL polarimetric radar. *J. Atmos. Oceanic. Technol.*, **21**, 1182-1189.

Larkin, R. P., 1991: Flight speeds observed with radar, a correction: slow "birds" are insects. *Behav. Ecol. Sociobiol.*, **29**, 221-4.

Lhermitte. R., 1990: Attenuation and scattering of millimeter wavelength radiation by clouds and precipitation. *J. Atmos. Ocean. Technol.*, **7**, 464-479.

Liu, S., Q. Xu, and P. Zhang, 2005: Identifying Doppler velocity contamination caused by migrating birds. Part II: Bayes identification and probability tests. *J. Atmos. Oceanic. Technol.*, **22**, 1114-1121.

Lowery, G. H. Jr. and R. J. Newman, 1966: A continentwide view of bird migration on four nights in Octorber. *The Auk,* **83**, 547-586.

Martin, W. J., 2003: *Measurements and Modeling of the Great Plains Low-Level Jet.* Ph.D. dissertation, University of Oklahoma, 243 pp. Available from University Microfilms, Ann Arbor, Michigan.

Martin, W. J. and A. Shapiro, 2005: Impact of radar tilt and ground clutter on wind measurements in clear air. *J. Atmos. Oceanic. Technol.,* **22**, 649-663.

Miller, P. A., M. F. Barth, J. R. Smart, and L. A. Benjamin, 1997: The extent of bird contamination in the hourly winds measured by the NOAA profiler network: results before and after implementation of the new bird contamination quality control check. Preprints*, 1st Symposium on Integrated Observing Systems*, Long Beach, CA., 138-144.

Mueller, E. A., 1983: Differential reflectivity of birds and insects. Preprints, *27th Conference on Radar Meteorology*. Edmonton, Canada, Amer. Meteor. Soc.

O'Bannon, T. 1995: Anomalous WSR-88D wind profiles—migrating birds? Preprints, *27th Conference on Radar Meteorology*, Vail, Colorado, Amer. Meteor. Soc.

Pekour, M. S. and R. L. Coulter, 1999: A technique for removing the effect of migrating birds in 915 MHz wind profiler data. *J. Atmos. and Oceanic. Tech.*, **16**, 1941-1948.

Probert-Jones, J. R., 1962: The radar equation in meteorology. *Quart. J. Roy. Meteor. Soc.,* **88**, 485-95.

Reynolds, D. R., J. W. Chapman, A.S. Edwards, A.D. Smith, C.R. Wood, J.F. Barlow, and I.P. Woiwod, 2005: Radar studies of the vertical distribution of insects migrating over southern Britain: the influence of temperature inversions on nocturnal layer concentrations. *Bull. Of Entomol. Res.*, **95**, 259-74.

Riley, J. R., 1975: Collective orientation in night-flying insects. *Nature*, **253**, 113-114.

Riley, J. R., 1985: Radar cross section of insects. *Proceedings of the IEEE,* **73**, 228-232.

Riley, J. R., 1989: Remote sensing in entomology. *Ann. Rev. Entomol.*, **34**, 247-271.

Russel, R. W. and J. W. Wilson, 1997: Radar-observed "fine lines" in the optically clear boundary layer: reflectivity contributions from aerial plankton and its predators. *Bound-Layer Meteor.*, **82**, 235-262.

Schaefer, G. W., 1976: Radar observations of insect flight. In *Insect Flight*, R. C. Rainey, ed. John Wiley & Sons, New York.

Shamoun-Baranes, J., E. van Loon, H. van Gasteren, J. van Belle, W. Bouten, and L. Buurma, 2006: A comparitive [sic] analysis of the influence of weather on the flight altitudes of

birds. *Bull. Amer. Meteor. Soc.*, **87**, 47-61.

Silverman, R. A., 1956: Turbulent mixing theory applied to radio scattering. *J. Appl. Phys.,* **27***,* 699-705.

Tatarski, V. I., 1961: *Wave Propagation in a Turbulent Medium.* Translated from Russian by R. A. Silverman. McGraw-Hill Book Company.

Van de Kamp, D. W., F. M. Ralph, M. F. Barth, P. A. Miller, J. R. Smart, and L. A. Benjamin, 1997: The new bird contamination quality control check applied to hourly winds from NOAA's profiler network. Preprints*, 28th Conference on Radar Meteorology*, Austin, TX, Amer. Meteor. Soc.

Vaughn, C. R., 1985: Birds and insects as radar targets: a review. *Proceedings of the IEEE,* **73***,* 205-227.

Wilczak, J. M., R. G. Strauch, F. M. Ralph, B. L. Weber, D. A. Merrit, J. R. Jordan, D. E. Wolfe, L. K. Lewis, D. B. Wuertz, J. E. Gaynor, S. A. McLaughlin, R. R. Rogers, and A. C. Riddle, 1995: Contamination of wind profiler data by migrating birds: characteristics of corrupted data and potential solutions. *J. Atmos. Oceanic Technol.*, **12**, 449-467.

Wilson, J. W., T. M. Weckwerth, J. Vivekanandan, R. M. Wakimoto, and R. W. Russell, 1994: Boundary layer clear-air radar echoes: origin of echoes and accuracy of derived winds. *J. Atmos. And Ocean. Tech.,* **11,** 1184-1206.

Wiscombe, W. J., 1979: *Mie scattering calculations: advances in technique and fast, vector-speed computer codes.* NCAR Technical Note NCAR/TN-140+STR, 64 pp., National Center for Atmospheric Research.

Wiscombe, W. J., 1980: Improved Mie scattering algorithms. *Applied Optics,* **19,** 1505-1509.

Wurman, J., 2001: The DOW mobile multiple Doppler network. Preprints *Thirtieth*

International Conf. on Radar Meteor., Munich, Germany, Amer. Meteor. Soc.

Wurman, J., J. Straka, E. Rasmussen, M. Randall, and A. Zahrai, 1997: Design and deployment of a portable, pencil-beam, pulsed 3-cm Doppler Radar. *J. Atmos. Oceanic. Technol.,* **14,** 1502-1512.

Zhang, P., S. Liu, Q. Xu, 2005: Identifying Doppler velocity contamination caused by migrating birds. Part I: feature extraction and quantification. *J. Atmos. Oceanic. Technol.*, **22**, 1105-1113.

Zhang, P., A. Ryzhkov, and D. Zrnić, 2005: Observations of insects and birds with a polarimetric prototype of the WSR-88D radar. *32nd Conference on Radar Meteorology*, Albuquerque, NM, Amer. Meteor. Soc.

Zrnić, D. S. and A. V. Ryzhkov, 1998: Observations of insects and birds with a polarimetric radar. *IEEE Trans. Geosci. and Remote Sens.*, **36**, 661-668.

Zrnić, D. S. and A. V. Ryzhkov, 1999: Polarimetry for weather surveillance radars. *Bull. Amer. Met. Soc.*, **80**, 389-406.

List of tables

Table 1. Selected characteristics of radars used in this study.

Table 2. Radar cross-section, σ, and effective dBZ values for a 3 cm radar for some insect and bird targets. For calculating dBZ_e **values,** the radar is assumed to have a 12 m gate spacing (as for DOW3) and a slant range to the target of 2 km. Cross-section values from Eastwood (1967), Riley (1985), and Vaughn (1985).

Table 1. Selected characteristics of radars used in this study.

	DOW3	WSR88-D	UMASS
Frequency (MHz)	9380	2700-3000	95040
Wavelength (cm)	3.198	10.0-11.1	.3157
Beam width (deg)	.95	.95	.18
Peak power (kW)	250	750	1.2
Antenna diameter (m)	2.44	8.5	1.2
Gate spacing (m)	12 – 600	250 (velocity)	15
		1000 (reflectivity)	
Pulse width (μs)	.075 – 2	1.57 and 4.7	.2

Table 2. Radar cross-section, σ, and effective dBZ values for a 3 cm radar for some insect and bird targets. For calculating dBZ_e **values,** the radar is assumed to have a 12 m gate spacing (as for DOW3) and a slant range to the target of 2 km. Cross-section values from Eastwood (1967), Riley (1985), and Vaughn (1985).

TARGET	*dBZ_e*	*σ, cm^2*
Birds	7 to 47 dBZ with 30 dBZ typical	10^{-1} to 10^{3} with 20 typical
Insects	-13 to 27 dBZ with 17 dBZ typical	10^{-3} to 10^{1} with 1 typical
Mosquito	-13 dBZ	10^{-3}
Sand piper	30 dBZ	20
Robin	30 dBZ	20
Locust	27 dBZ	1
Moth	17 dBZ	1
Butterfly	7 dBZ	10^{-1}

List of figures

Figure 1. Time-height cross-section of reflectivity through a depth of 4 km and for 24 hours from KVNX radar, 1-2 June 2002. 1.5° tilt. Data begins at 1605 UTC 1 June (LST is 6 hours earlier than UTC). Contour increment is every 2 dBZ. Vertical lines indicate the time of sun set and rise.

Figure 2. Base 10 logarithm of radar cross-section in cm^2 as a function of water sphere radius at 20°C for 3 mm, 3 cm, and 10 cm radars; from Mie scatter calculations. Three parallel thick solid lines are the Rayleigh scatter approximations. Thick solid line crossing the three parallel lines is the line for which the radar cross-section equals the actual spherical cross-section. The letters "R", "I", and "B" are plotted at the approximate equivalent water sphere sizes for rain drops, insects, and birds, respectively.

Figure 3. PPI scans for (left) KGLD and (right) DOW3 radars both at 30 May 2000 0600 UTC. For KGLD, gate spacing was 1 km; gray scale range is from -15 dBZ (white) to 15 dBZ (black). For DOW3, gate spacing was 137 m and gray scale range is from -30 dBZ (white) to 0 dBZ (black). Distance scale is the same for both images, with range rings being drawn every 200 m above the ground. The total horizontal range is 45 km. A box is drawn in the lower left region of each figure around an area analyzed for reflectivity.

Figure 4. PPI reflectivity scan from DOW3 with a 12 m gate spacing, obtained on 30 May 2000 at 0608 UTC with a 10° elevation. Dark arcs and lines are ground clutter. Reflectivity scale is

from -20 dBZ (white) to 10 dBZ (black). Range rings are drawn every 50 m in elevation. Total horizontal range is 3 km.

Figure 5. Reflectivity RHI scan from DOW3 at Goodland, KS on 30 May 2000 at 0548 UTC. Range rings are drawn every 200 m in range. Gray scale is from -20 dBZ (white) to 10 dBZ (gray). Arc echoes near radar are from ground clutter.

Figure 6. PPI scan of reflectivity from KTLX on 19 May 2001 near 0400 UTC. Antenna elevation was 1.5°. Range rings are drawn every 0.25 km of height above the ground. Total horizontal range is 95 km. Reflectivity scale is from 0 dBZ (white) to 25 dBZ (black).

Figure 7. Wind speed profile derived by VAD analysis of KTLX radial velocity data from the same volume scan as Fig. 8.

Figure 8. Time-height display for reflectivity from UMASS radar at Norman, OK. The time was about 0400 UTC 19 May 2001. Vertical lines are drawn every 10 seconds and horizontal lines are drawn every 200 m. Total depth displayed is 3 km and total time is 195 s. Reflectivity scale is from -30 dBZ (white) to -15 dBZ (black).

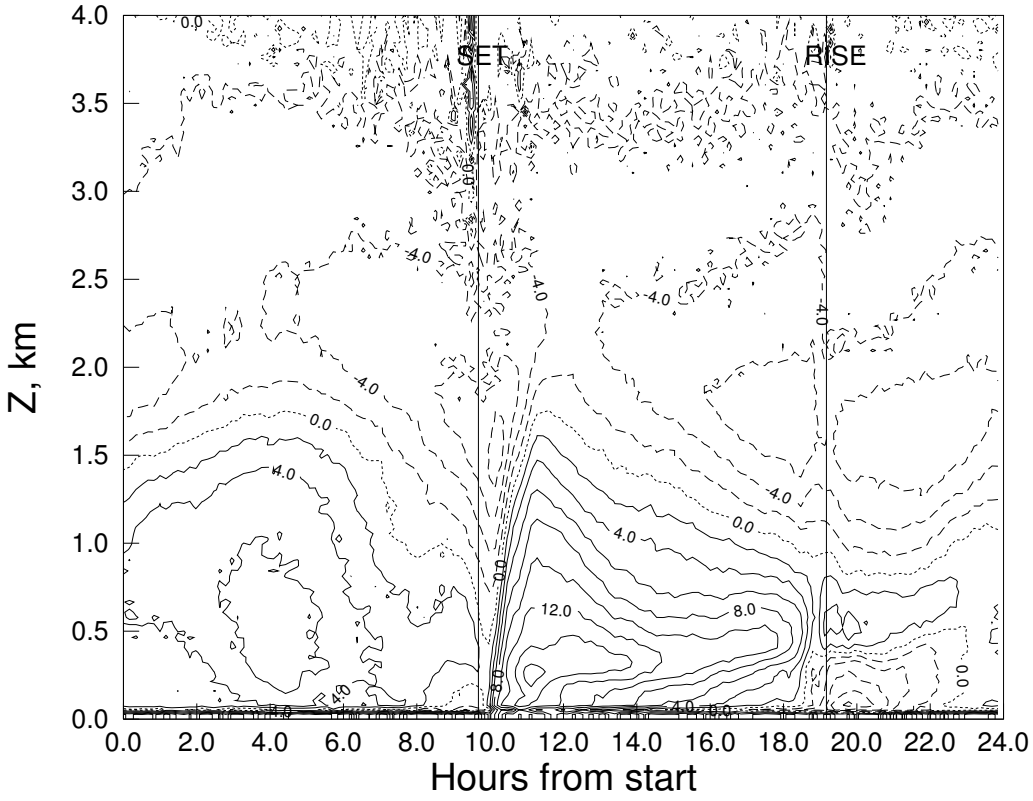

Figure 1. Time-height cross-section of reflectivity through a depth of 4 km and for 24 hours from KVNX radar, 1-2 June 2002. 1.5° tilt. Data begins at 1605 UTC 1 June. (LST is 6 hours earlier than UTC). Contour increment is every 2 dBZ. Vertical lines indicate the time of sun set and rise.

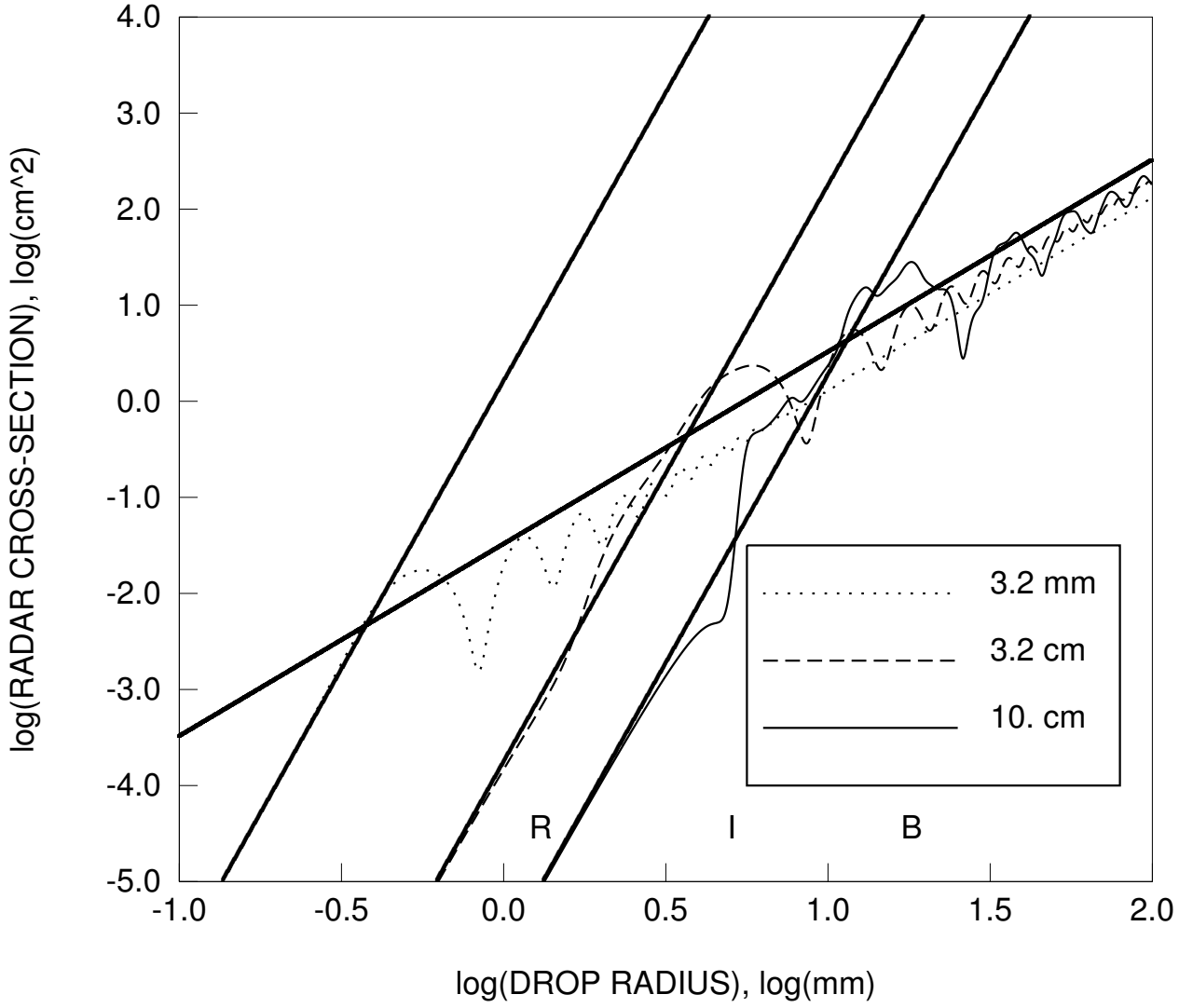

Figure 2. Base 10 logarithm of radar cross-section in cm^2 as a function of water sphere radius at 20°C for 3 mm, 3 cm, and 10 cm radars; from Mie scatter calculations. Three parallel thick solid lines are the Rayleigh scatter approximations. Thick solid line crossing the three parallel lines is the line for which the radar cross-section equals the actual spherical cross-section. The letters "R", "I", and "B" are plotted at the approximate equivalent water sphere sizes for rain drops, insects, and birds, respectively.

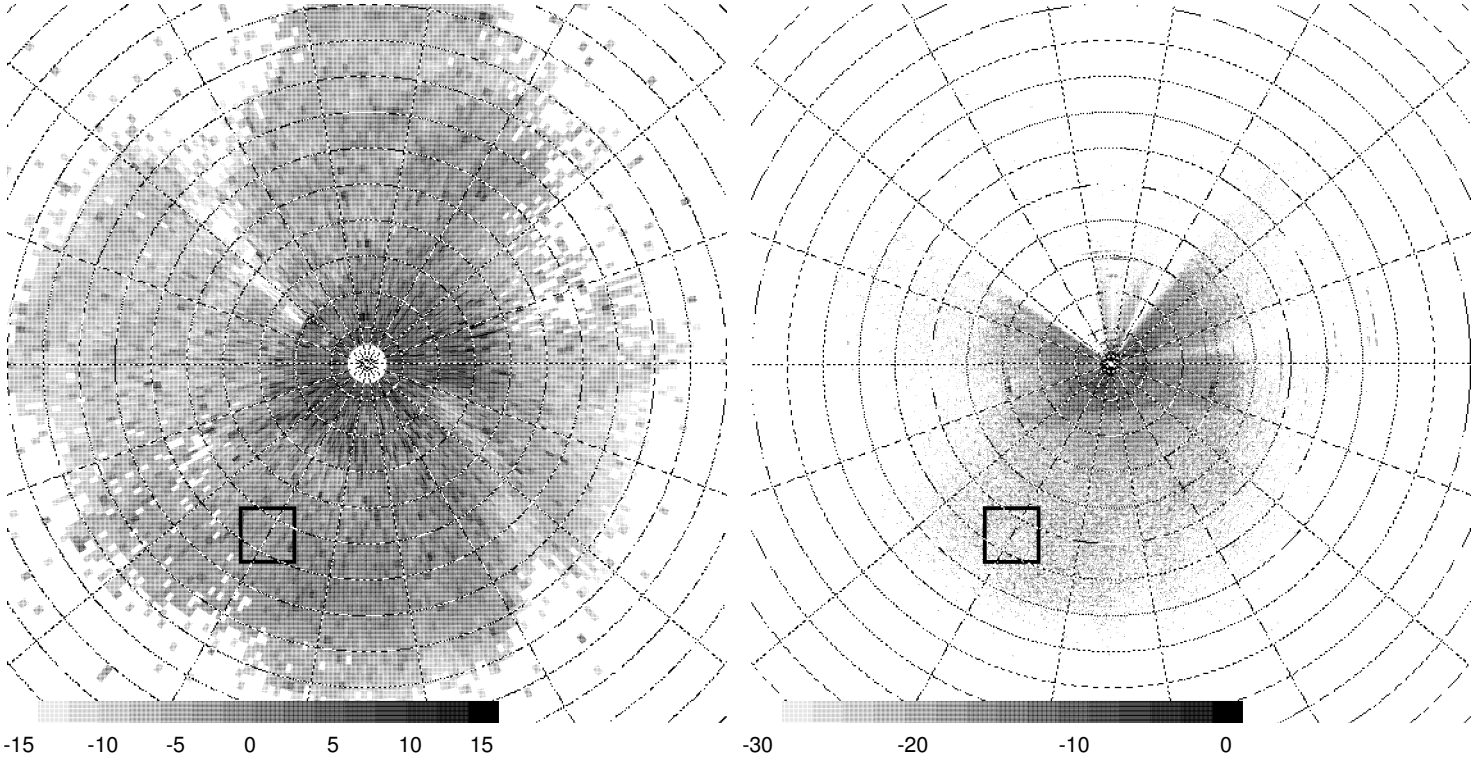

Figure 3. PPI scans for (left) KGLD and (right) DOW3 radars both at 30 May 2000 0600 UTC. For KGLD, gate spacing was 1 km; gray scale range is from -15 dBZ (white) to 15 dBZ (black). For DOW3, gate spacing was 137 m and gray scale range is from -30 dBZ (white) to 0 dBZ (black). Distance scale is the same for both images, with range rings being drawn every 200 m above the ground. The total horizontal range is 45 km. A box is drawn in the lower left region of each figure around an area analyzed for reflectivity.

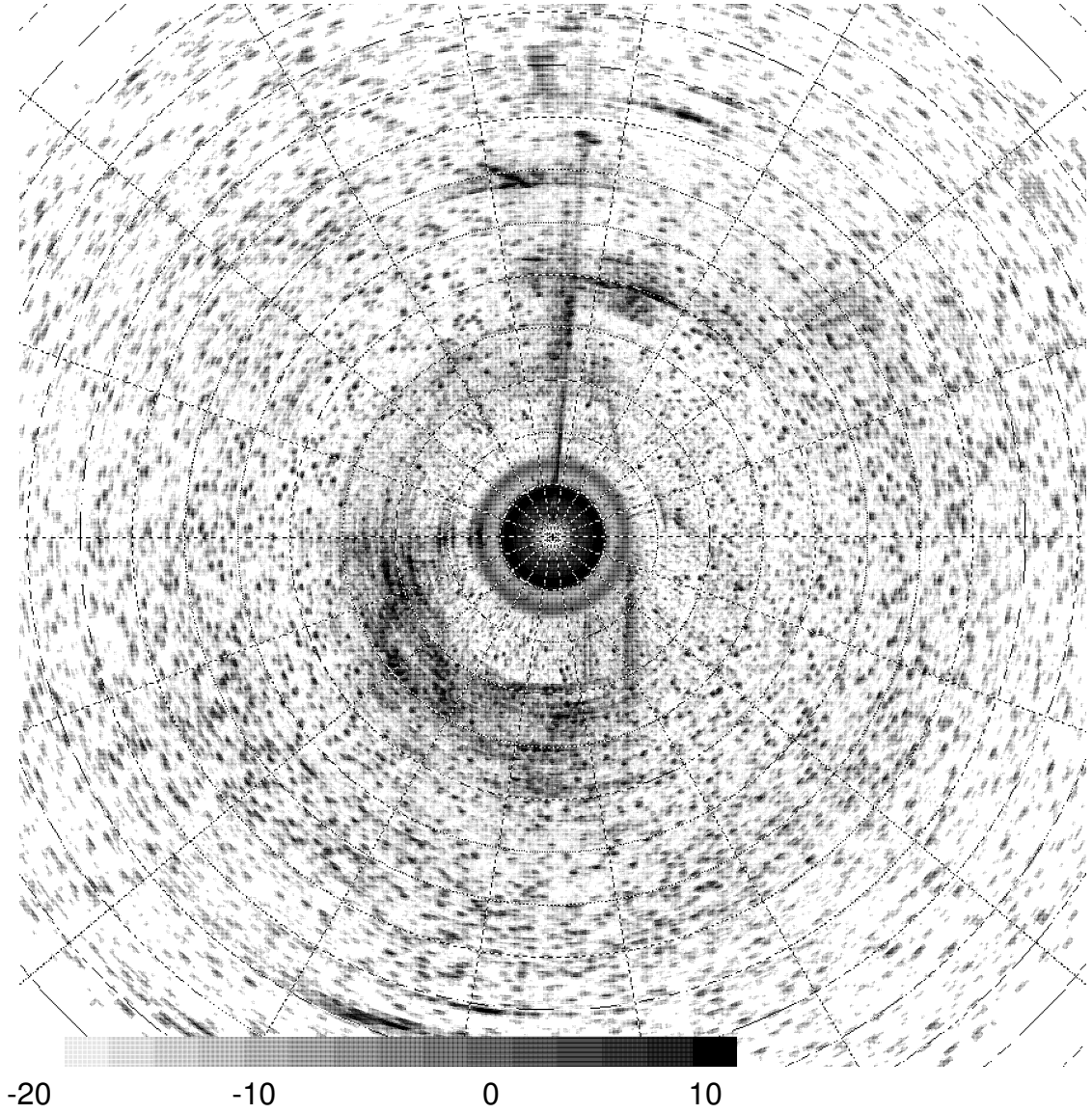

Figure 4. PPI reflectivity scan from DOW3 with a 12 m gate spacing, obtained on 30 May 2000 at 0608 UTC with a 10° elevation. Dark arcs and lines are ground clutter. Reflectivity scale is from -20 dBZ (white) to 10 dBZ (black). Range rings are drawn every 50 m in elevation. Total horizontal range is 3 km.

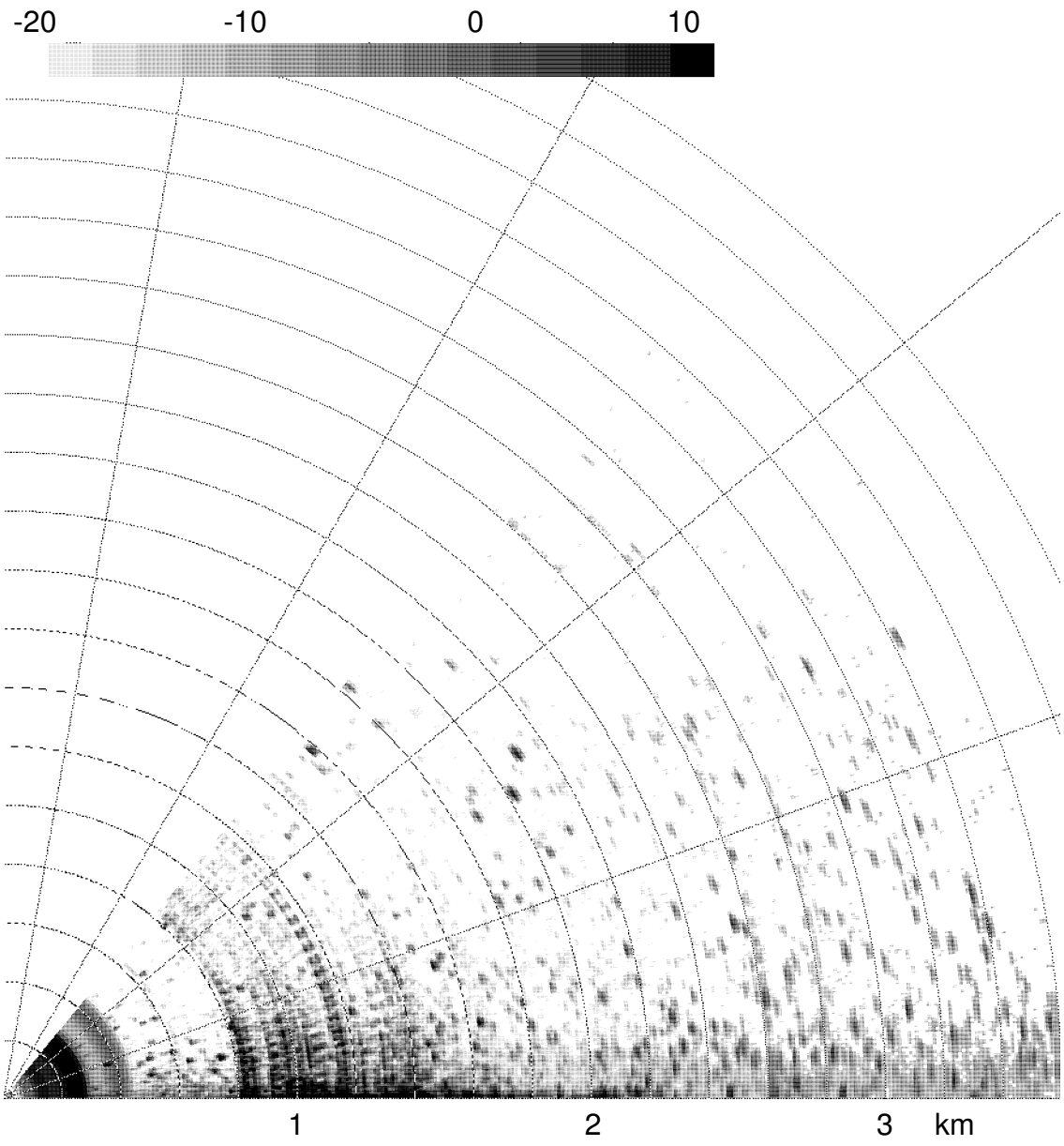

Figure 5. Reflectivity RHI scan from DOW3 at Goodland, KS on 30 May 2000 at 0548 UTC. Range rings are drawn every 200 m in range. Gray scale is from -20 dBZ (white) to 10 dBZ (gray). Arc echoes near radar are from ground clutter.

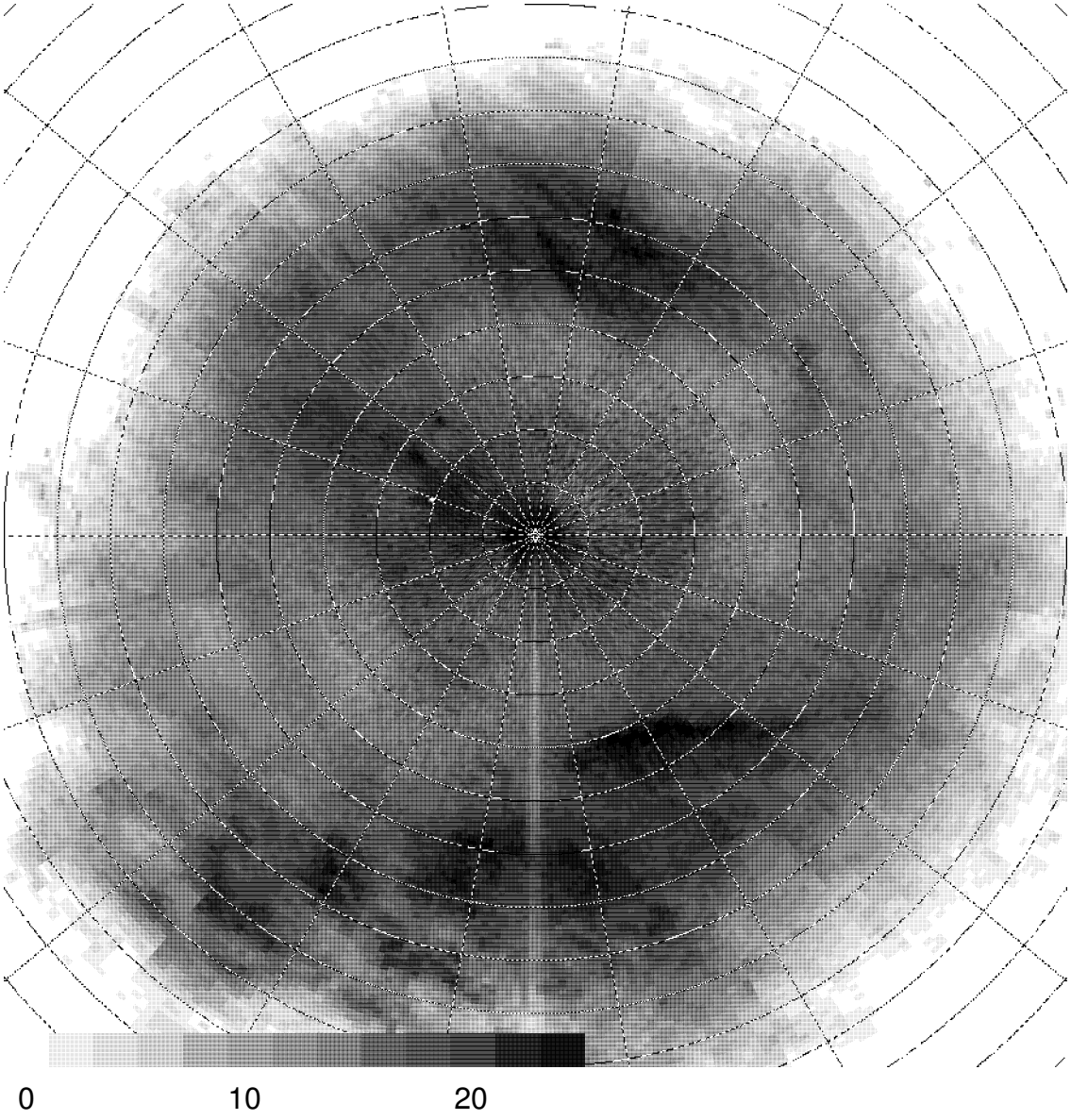

Figure 6. PPI scan of reflectivity from KTLX on 19 May 2001 near 0400 UTC. Antenna elevation was 1.5°. Range rings are drawn every 0.25 km of height above the ground. Total horizontal range is 95 km. Reflectivity scale is from 0 dBZ (white) to 25 dBZ (black).

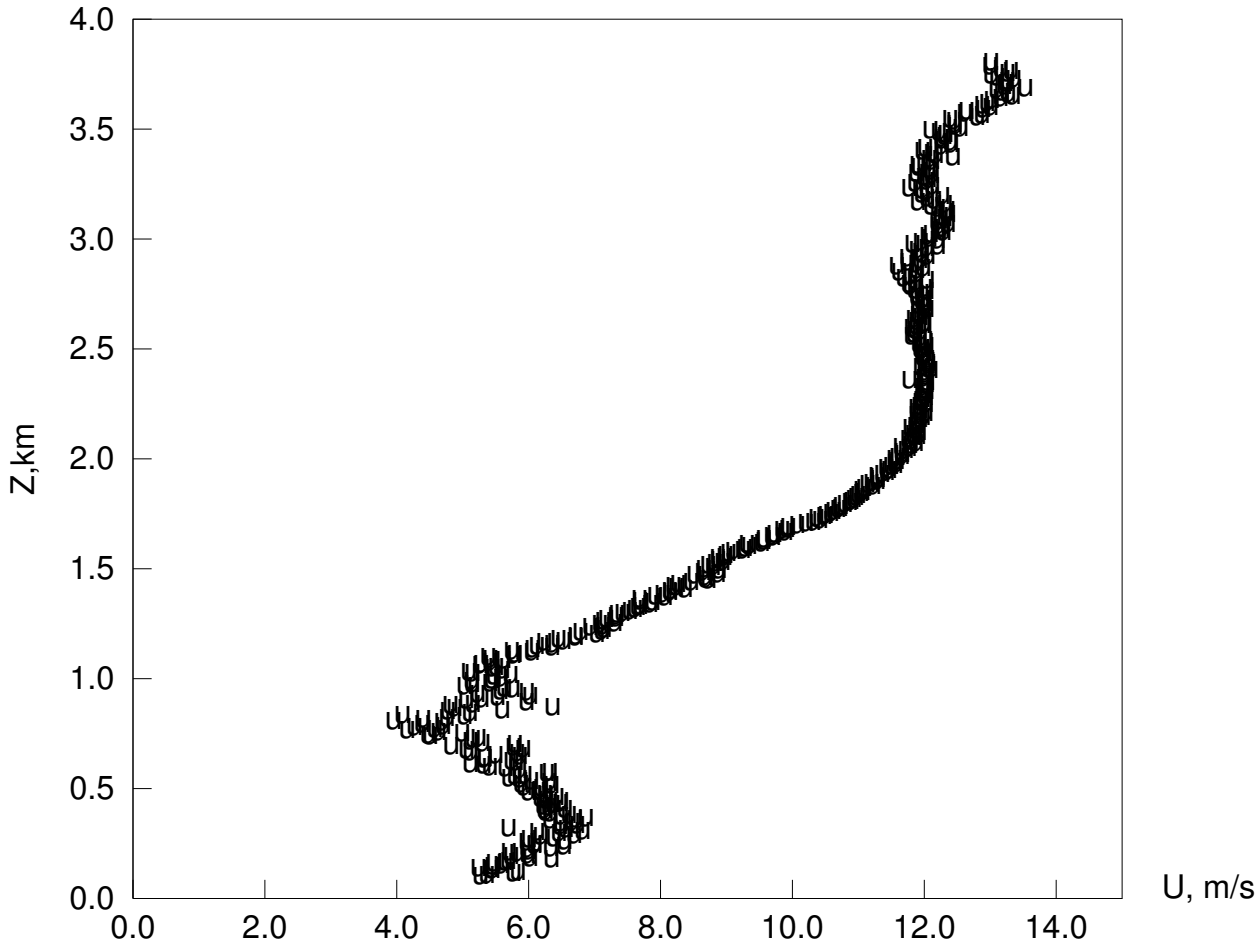

Figure 7. Wind speed profile derived by VAD analysis of KTLX radial velocity data from the same volume scan as Fig. 8.

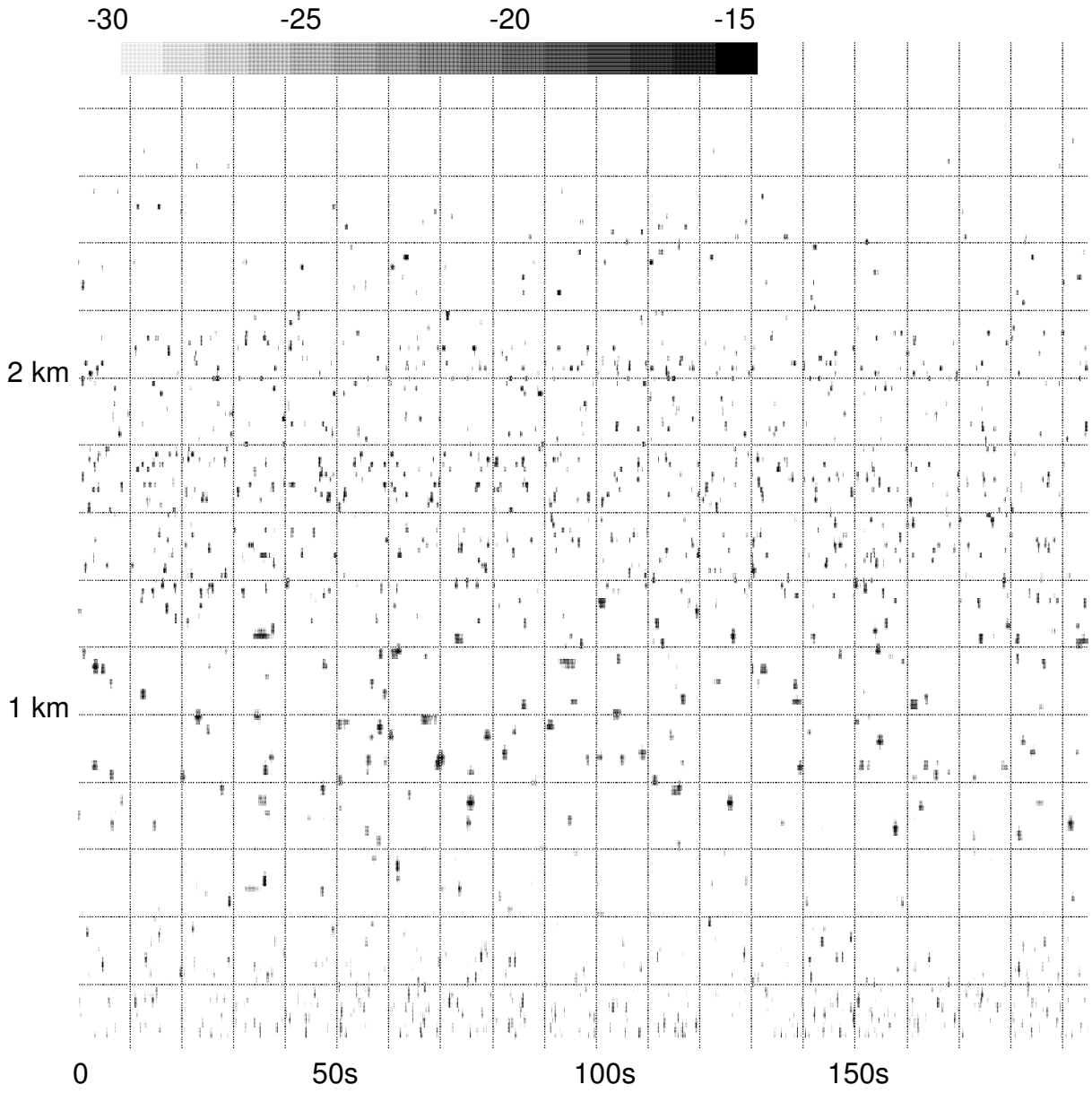

Figure 8. Time-height display for reflectivity from UMASS radar at Norman, OK. The time was about 0400 UTC 19 May 2001. Vertical lines are drawn every 10 seconds and horizontal lines are drawn every 200 m. Total depth displayed is 3 km and total time is 195 s. Reflectivity scale is from -30 dBZ (white) to -15 dBZ (black).